Optical tweezers and confocal microscopy for simultaneous three-dimensional manipulation and imaging in concentrated colloidal dispersions

Dirk L. J. Vossen[a] and Astrid van der Horst
FOM Institute for Atomic and Molecular Physics, Kruislaan 407, 1098 SJ Amsterdam, and Soft Condensed Matter, Debye Institute, Utrecht University, Princetonplein 5, 3584 CC Utrecht, The Netherlands

Marileen Dogterom
FOM Institute for Atomic and Molecular Physics, Kruislaan 407, 1098 SJ Amsterdam, The Netherlands

Alfons van Blaaderen[b]
FOM Institute for Atomic and Molecular Physics, Kruislaan 407, 1098 SJ Amsterdam, and Soft Condensed Matter, Debye Institute, Utrecht University, Princetonplein 5, 3584 CC Utrecht, The Netherlands

A setup is described for simultaneous three-dimensional manipulation and imaging inside a concentrated colloidal dispersion using (time-shared) optical tweezers and confocal microscopy. The use of two microscope objectives, one above and one below the sample, enables imaging to be completely decoupled from trapping. The instrument can be used in different trapping (inverted, upright, and counterpropagating) and imaging modes. Optical tweezers arrays, dynamically changeable and capable of trapping several hundreds of micrometer-sized particles, were created using acousto-optic deflectors. Several schemes are demonstrated to trap three-dimensional colloidal structures with optical tweezers. One combined a Pockels cell and polarizing beam splitters to create two trapping planes at different depths in the sample, in which the optical traps could be manipulated independently. Optical tweezers were used to manipulate collections of particles inside concentrated colloidal dispersions, allowing control over colloidal crystallization and melting. Furthermore, we show that selective trapping and manipulation of individual tracer particles inside a concentrated dispersion of host particles is possible as well. The tracer particles had a core–shell geometry with a high refractive index material core and a lower index material shell. The host particles consisted of the same material as the lower index shells and were fluorescently labeled. The tracer particles could be manipulated without exerting forces on the host particles because the mixture was dispersed in a solvent with the same refractive index as that of the host particles. Using counterpropagating tweezers strongly scattering particles that could not be trapped by conventional single-beam optical tweezers were trapped and manipulated. © *2004 American Institute of Physics.* [DOI: 10.1063/1.1784559]

I. INTRODUCTION

Since the invention of optical tweezers by Ashkin and co-workers[1,2] optical tweezers have found widespread use in fields like biology, physical chemistry, and (bio-) physics.[3–6] An optical trap can be created by focusing a laser beam to a diffraction-limited spot using a high numerical aperture (NA) objective. The strong light gradient near the focus creates a potential well, in which a particle with a refractive index higher than that of the surrounding medium is trapped. The forces on a particle can be decomposed into a "gradient force" in the direction of highest light intensity and a "scattering force" directed along the optical axis. The particle is trapped at the point where these two force contributions balance, if the maximal restoring force of the trap is large enough to overcome effective weight and thermal fluctuations of the particle. The general calculation of the optical forces on a particle in a trap is a challenging problem.[7] This task is simpler in the regimes where a particle is either much smaller[8] (Raleigh) or much larger[9] (ray optics) than the wavelength used for trapping. Dielectric particles, small metal particles as well as living materials, with sizes ranging from several nanometers to tens of micrometers, can be trapped and manipulated in a single beam gradient trap as long as the scattering force is not too large. If there is no difference in refractive index between the particle and its surroundings, there are no direct optical forces exerted on the particle. If the refractive index of the particle is lower than that of the medium, the particle is expelled from the trapping beam. However, alternative schemes such as rapid beam scanning[10] and the use of light beams with a phase singularity,[11] have been invented to manipulate particles in this situation. Recent developments have broadened the kind of forces that can be exerted onto small objects to include bending,[12] torques,[13,14] and stretching.[15]

To manipulate more than one particle at once, a number

---

[a]Electronic mail: d.l.j.vossen@phys.uu.nl
[b]Electronic mail: a.vanblaaderen@phys.uu.nl and www.colloid.nl

of methods have been developed to create and manipulate planar arrays of optical traps using galvano[16] or piezo-electric[17] scanning mirrors, acousto-optic deflectors (AODs),[3] (computer generated) diffractive optical elements,[18–21] interference of specially designed light beams,[22,23] or the generalized phase contrast method.[55]

Around the same time the single beam optical tweezers were pioneered, the confocal microscope was reinvented after it was first demonstrated at the end of the 1950s.[24,25] At present, confocal microscopy is widely used in biology and medicine, and its use in chemistry, physics, and materials science is increasing.[26–28] In confocal microscopy the sample is illuminated with a diffraction-limited spot while detection occurs by imaging the focal region with the same objective onto a pinhole aperture. Only a thin section of the sample contributes to the signal, thus out-of-focus stray light is efficiently reduced by the detection pinhole. By for instance scanning the beam in the sample a three-dimensional image can be build up. Besides the sectioning capability the use of pinholes also leads to an increase in resolution compared to conventional microscopy.[29]

Because of their tunability, in size, shape, as well as in chemical composition, and their ability to self-organize, colloids find applications in the development of advanced materials like photonic crystals.[30] In addition, colloidal systems are used as a model system in condensed matter.[31–33] Colloids have, like atoms, a well-defined thermodynamical temperature, their interaction potential is tunable, and the time and length scales involved are experimentally accessible. Recent developments in particle synthesis and labeling of particles with fluorescent dyes opened up the possibility to perform quantitative three-dimensional analysis using confocal microscopy on a single particle level.[34] Examples are experiments investigating the glass transition[35] and nucleation and growth of crystals[33,36] in colloidal dispersions. Optical tweezers have been used to manipulate colloidal particles, to pattern substrates with two- and three-dimensional structures,[37,38] and to measure double layer repulsions,[39] depletion,[40] and hydrodynamic interactions.[41] However, as selective manipulation in a concentrated dispersion was not possible until now, all applications have been limited to systems that were either (almost) two dimensional[31,42] or had a very low particle concentration.[23,43]

Combining the powerful techniques of optical tweezers and confocal microscopy opens up series of new experiments. For example, three-dimensional structures can be created with optical tweezers that can be imaged and studied in detail in three dimensions. In addition, their effect on other particles, which are not trapped, can be analyzed in three dimensions. The setup described in this article is designed to use optical tweezers and independently image the sample using confocal microscopy because it uses two microscope objectives on each side of the sample.

The simplest way of combining optical tweezers with a confocal microscope is by using the same objective to image and trap. However, this makes it impossible to use the three-dimensional scanning ability, and only one plane is imaged.[44] Hoffmann and co-workers implemented optical trapping and three-dimensional imaging using one objective and fast scan-

ning compensating optics to keep the tweezers at a fixed position.[45] The use of two independent microscope objectives for trapping and imaging was pioneered by Visscher and co-workers,[12,46] although trapping was limited to a two-dimensional plane. In this article we also use two microscope objectives, one above and one below the sample, to decouple imaging and trapping completely. Samples could be imaged quantitatively in three dimensions without affecting optical trapping performance. AODs were used to create large two-dimensional arrays of traps that could be changed dynamically. Three-dimensional arrays of traps were created by fast switching between two beam paths using AODs, a Pockels cell, and polarizing beam splitters.

We extended the use of optical tweezers in soft condensed matter systems to concentrated dispersions, both on an individual particle level using core–shell tracers and on collections of particles. We induced crystallization in a concentrated dispersion and demonstrated that selective trapping of core–shell tracer particles inside a concentrated dispersion of index matched host particles in combination with three-dimensional imaging is possible. Some preliminary results were described in Ref. 32. Using counterpropagating beams[1,47] we trapped high refractive index particles that were not stably trapped in a single beam gradient trap.

The remainder of the article is organized as follows. The next section describes the setup used to create the different trapping and imaging modes and it describes the colloidal dispersions used. In Sec. III we demonstrate the flexibility, accuracy, and speed of AODs to create large arrays of optical traps which can be changed dynamically. In Secs. IV and V decoupled trapping and imaging, and arrays of tweezers created in more than one plane are demonstrated. How optical tweezers can be used in concentrated colloidal dispersions is demonstrated in Sec. VI while Sec. VII shows the use of counterpropagating tweezers for trapping high index particles. We end with conclusions and an outlook.

II. EXPERIMENT

A. Upright, inverted, and counterpropagating optical tweezers arrays

Figure 1 shows a schematic drawing of the setup. We use a diode-pumped Nd:YVO$_4$ laser (Spectra Physics, Millennia IR, 10 W, cw) with a wavelength of 1064 nm and a TEM$_{00}$ mode profile. The wavelength was chosen such that it is well separated from the excitation and emission wavelengths of the fluorescent dyes used in the confocal microscopy modes. This wavelength also minimizes absorption and scattering in biological materials. The laser beam is expanded six times using a beam expander (*EXP*, Melles Griot). The beam is attenuated using a half-lambda zero-order wave plate (*W*1, Newport), which rotates the vertically polarized laser light, in combination with a polarizing beam splitter cube (*C*1). The horizontally polarized fraction is directed into a beam dump.

Using a gimbaled mirror (*M*1, Newport), the vertically polarized beam is coupled into two AODs (IntraAction Corp., DTD-276HB2, 6×6 mm^2 aperture). In the AODs a diffraction grating is set up by a sound wave propagating
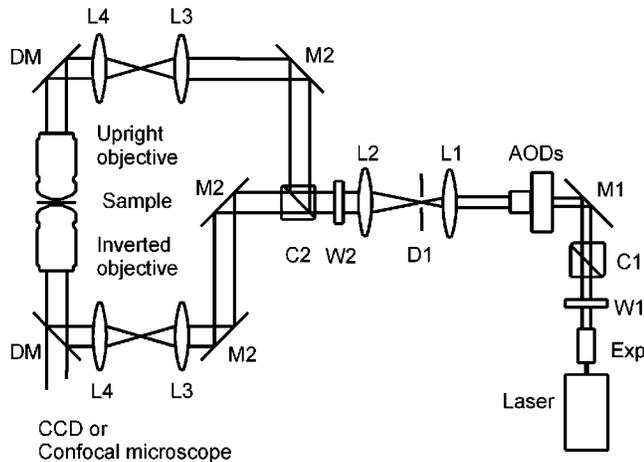
FIG. 1. Schematic diamgram of the setup used to create inverted, upright, and counterpropagating optical tweezers. Two objectives allowed imaging to be completely decoupled from trapping. AODs were used for beam steering and the creation of arrays of tweezers.

through the TeO_2 crystals. The laser beam is deflected at specific angles and intensities that depend on the frequency and the amplitude of the sound wave in the crystal, respectively. We corrected, if needed, for the diffraction efficiency of the AODs not being constant over the frequency range by either adjusting the amplitude of the signal to the AODs or by changing the relative time spent by the laser beam at a certain frequency.

A synthesizer board and amplifier (both IntraAction Corp.) allow for fast and accurate control over the position as well as the stiffness of the optical trap. The synthesizer board was controlled using a *LabVIEW* (National Instruments) program, which addressed a *C++* program when faster switching was needed. The beam is scanned quickly from point to point in the sample using the AODs to create arrays of tweezers with great control over the position of the traps. We also used direct digital synthesizers (Novatech Instruments Inc., DDS8m 100 MHz) to create multiple traps without timesharing the laser beam. Two frequencies were applied simultaneously to the AODs, resulting in a corresponding number of diffracted beams. With this procedure, the beams are not time-shared and can be modulated independently although the intensities are interrelated.

The two AODs are each fitted on a four-axis kinematic stage (New Focus) for better alignment. As the AODs diffract the incoming laser into multiple beams, a diaphragm ($D1$) is used to select the (1,1) order for trapping. By careful alignment of the AODs with respect to the incoming laser beam, up to 60% of the light of the original undiffracted beam can be transferred into the (1,1) order.

The deflected beam is broadened further using a telescope with lenses $L1(f=120 \text{ mm})$ and $L2(f=250 \text{ mm})$. All lenses are achromat doublets and were obtained from Melles Griot while the mirrors and beam-splitting cubes were from Newport. All components have an antireflection coating for 1064 nm. The combination of the telescope and the beam expander broadens the laser beam 12 times to a width of $2\omega_0=5.6 \text{ mm}$, equal to the back aperture of the $100\times$ objective.

Switching between different trapping modes is done using a half-lambda wave plate $W2$ combined with a polarizing beam splitter cube $C2$. Rotation of the wave plate determines the fraction of the beam diverted to the upper or the lower beam paths, thereby switching between inverted and upright trapping modes. When both paths are used at the same time, inverted and upright single beam optical traps can be created at different heights in the sample. Dual-beam counterpropagating optical tweezers can be created when the inverted and upright tweezers are aligned on top of each other. Depending on whether the lower or the upper beam path is used, the scattering force augments or counteracts gravity.

Mirrors ($M2$) and the 1:1 telescope lenses ($L3$ and $L4$, both $f=80 \text{ mm}$) guide the beam to the microscope. The lenses $L3$ are placed on *xyz* stages fitted with micromanipulators. The lenses $L3$ as well as the AODs are positioned in planes conjugate to the back focal plane of the objectives. This allows for manipulation of the optical traps in the front focal plane of the objective by changing the angle at which the beam enters the back aperture of the microscope objective. The lenses $L3$ are achromat doublet lenses to minimize aberrations. Also the displacement of these lenses from the optical axis is small and we have not seen any notable change in trap efficiency when lenses $L3$ were moved. For optimal two-dimensional position control, the AODs are aligned such that the plane between the two AODs is conjugate to the backfocal planes of the two objectives. The distance between the centers of the AODs is 32 mm.

Two dichroic mirrors (DM, ChromaTech) are attached to the body of an inverted microscope (Leica, DMIRB). The mirrors reflect the 1064 nm laser beam into the back aperture of the objectives while they allow imaging in the visible. The revolver of the microscope is replaced with a block holding the inverted objective, and the condenser is replaced by the upper microscope objective. This upright objective is mounted on an *xyz* translation stage, fitted with microscrews (Newport), for manipulation and alignment. The upright objective can be used as a condenser for imaging as well as for trapping. We used $100\times(0.7-1.4 \text{ NA})$, $63\times(1.4 \text{ NA})$, and $40\times(1.4 \text{ NA})$ oil immersion objectives and a $20\times(0.7 \text{ NA})$ air objective. All objectives were plan apochromats and were obtained from Leica.

A high-resolution piezo stage (Physik Instrumente, P-730.4C, accuracy better than 0.5 nm when operated in a closed loop circuit) is mounted on the body of the microscope, providing the ability to move the sample with high accuracy. The power of the laser was measured using a broadband power meter (Melles Griot). The setup was built on a vibration–isolation table (Melles Griot).

B. Arrays of tweezers in more than one plane using one objective

To create multiple traps in different planes and to image the sample in three dimensions simultaneously, the laser beam was split into two beams, which were recombined after changing their relative divergence. As the (*z* axis) position of the trapping plane is determined by the divergence (or convergence) of the beam at the back focal plane of the objective, we were able to create traps in two different planes in
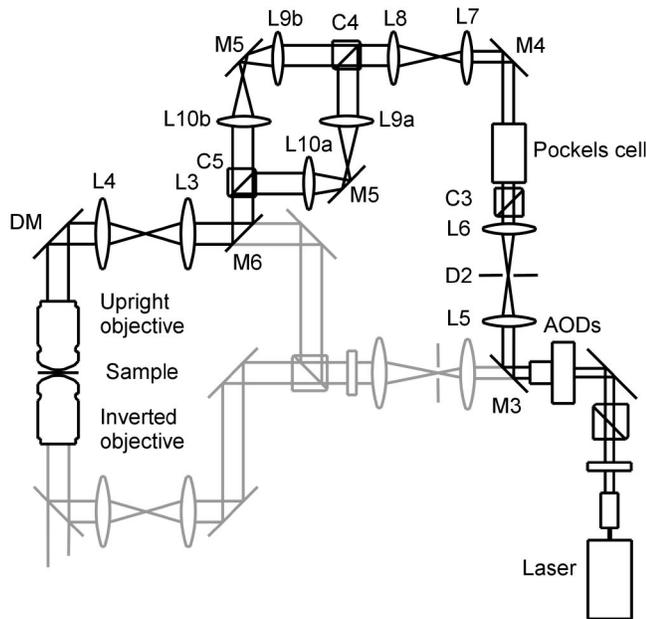
FIG. 2. Setup used for the creation of arrays of tweezers in two trapping planes. A Pockels cell and beam splitting cubes (C4 and C5) were used to switch between the planes. The Pockels cell and the AODs were synchronized to create different arrays of traps in each plane. The upright objective was used for trapping, while the inverted objective was used for imaging. The part of the setup drawn in light gray was not used when two trapping planes were created.

the sample. Switching between these planes can be done using a Pockels cell, which rotates the polarization of the laser beam, combined with a polarizing beam splitting cube. Synchronizing the Pockels cell with the AODs creates independent arrays of optical tweezers.

Figure 2 shows the setup used for creating arrays of tweezers in two separate planes. A mirror ($M3$) after the AODs reflects the beam into a 1:1 telescope formed by two lenses ($L5$ and $L6$, both $f=120$ mm). A polarizing beam splitting cube ($C3$) is placed in front of the Pockels cell (Conoptics, 360-50 LA) to remove any horizontal component of the polarization introduced by the AODs. A personal computer with an analog output board (NuDAQ PCI-6208V) controls the angle of rotation of the polarization induced by the Pockels cell. The computer also contains the synthesizer board that generates the acoustic signals for the AODs. Both boards are controlled and synchronized using a *LabVIEW* program to create independent arrays in each trapping plane. For increased speed, the *LabVIEW* program calls a *C++* program to write the data to the two boards.

After the Pockels cell and a mirror ($M4$), the lenses $L7$ and $L8$ ($f=65$ and 140 mm) expand the beam to overfill the back aperture of the objective. A polarizing beam splitter cube ($C4$) splits the laser beam into two separate paths. In each of the paths the beam passes through a 1:1 telescope formed by a pair of lenses ($L9a,b$ and $L10a,b$ all $f=90$ mm). The lenses $L9a,b$ are positioned in a plane conjugate to the back focal plane of the upright objective. The lens $L9a$ is mounted on an xyz translation stage allowing displacement of the traps created in the sample with path a with respect to the traps created with path b. After recombination of the two beams using a polarizing beam splitter

cube ($C5$), the combined beam is coupled into the microscope with the mirrors $M5$, $M6$ and lenses $L3$ and $L4$. A movement of lens $L3$ results in a collective displacement of the traps created with paths a and b. The lenses $L3$ and $L9a,b$ as well as the Pockels cell and the AODs are all in planes conjugate to the back focal plane of the upright objective. Because of the length of the Pockels cell (75 mm) and the small aperture (5×5 mm²), the modulator is placed with its center at a plane conjugate to the back focal plane of the objective. The mirrors $M3$ and $M6$ are placed on flippers (New Focus) to move them out the beam path when this part of the setup was not used.

C. Imaging modes

The inverted objective is used for imaging while both the inverted and upright objectives can be used for trapping. The sample can be imaged in bright field, differential interference contrast (DIC), epifluorescence, and reflection microscopy using mercury or halogen light sources. For DIC imaging, a polarizer and Wollaston prism are placed below the inverted objective in addition to an analyzer and a prism placed above the upright objective. The sample is imaged with a charge coupled device (CCD) camera (UNIQ, UP-600), which is read out by a home built frame grabber using a programmable coprocessor (SiliconSoftware, microEnable). The images (540×480 pixels, 10 bit grayscale) can be stored digitally on an array of hard disks (Promise tech., Fasttrak100) at a rate of 20 Hz for full images and up to 50 Hz for smaller regions. For position detection in real time, the frame grabber is programmed to determine the gray-value center of mass of particles separated by at least a line of pixels on the CCD. An infrared filter (Schott) is used to block the trapping beam from the CCD camera.

For confocal imaging we use a commercial confocal scan head (Leica TCS NT) attached to the side port of the inverted microscope. The confocal microscope excites the sample using a mixed-gas Kr/Ar laser, and the fluorescence is detected using photomultiplier tubes. To image the sample in three dimensions, the lower objective is mounted on a microscope objective scanner (Physik Instrumente, Pifoc P-721.20) operated in closed loop mode, while the sample is kept stationary. The software of the confocal microscope controls the piezo driver electronics. For imaging of the fluorescently labeled silica particles described in the next section, the 488 nm line of the Kr–Ar laser was used in combination with cutoff filters. The silica-coated polystyrene particles were imaged in reflection mode using a second photomultiplier tube. Only in the upright mode and at high powers was the trapping laser detected by the photomultiplier tubes. In that case an infrared filter was used to block the trapping laser from the imaging channels that were used in the visible. Image analysis was done using routines similar to those described in Refs. 34 and 48.

D. Colloidal dispersions

Colloidal silica particles with a core–shell geometry were synthesized using the so-called Stöber growth process, modified to incorporate a fluorescent dye and followed by a

seeded growth. This method and particle characterization are described in more detail elsewhere.[49–51] We used two sizes of silica particles with average diameters of 1384 and 1050 nm and polydispersities of 1.5% and 3%, respectively. The diameters of the cores were determined to be 386 and 400 nm, respectively, and the cores were labeled with the fluorescent dye fluorescein isothiocyanate (FITC). We will refer to the fluoresceine labeled silica particles as FITC–SiO_2. ZnS particles were synthesized following a procedure described elsewhere.[52] The ZnS particles had an average diameter of 500 nm and a polydispersity of 10%. The index of refraction of the ZnS particles was estimated[52] to be $n_D^{20}=2.0$.

Recently, we developed a method to synthesize core–shell particles with a polystyrene core and a silica shell.[53] Polyvinyl pyrrolidone (PVP) was absorbed onto polystyrene (PS) particles with a diameter of 772 nm (estimated refractive index $n_D^{20}=1.6$), and then a silica shell was grown onto the PVP-coated PS particles in several growth steps. The final diameter of the particles was determined to be 975 nm with a polydispersity of less than 3%. We will refer to the polystyrene–silica core–shell particles as PS–SiO_2. The densities of the particles used are not important for the trapping experiments in this article as optical forces exceed gravitational force by far. The densities of the particles used are stated in cited references.

The particles were dispersed in ethanol (Merck, analytical grade), dimethyl formamide (DMF) (Merck, analytical grade), or a mixture of DMF and dimethylsulfoxide (DMSO) (Merck, analytical grade). All chemicals were used as received.

In order to match the refractive index of the FITC–SiO_2 particles, we made a series of solvent mixtures with different relative composition of DMF and DMSO but with a constant concentration of silica particles. For each mixture the transmission was measured at a wavelength of 1064 nm using a spectrometer (Perkin Elmer). A mixture with a volume ratio of DMF:DMSO=18%:82% was found to index match the particles at 1064 nm. Using an Abbe refractometer (Atago, 3T), the refractive index of the matching mixture was measured to be $n_D^{20}=1.4675$. For the trapping experiments on particles in a concentrated dispersion, a small amount of PS–SiO_2 particles was added to a concentrated dispersion of FITC–SiO_2 particles. The mixture was then transferred to a refractive index matching mixture of DMF and DMSO in several centrifugation (not exceeding 120 g) and redispersion steps.

Samples with a thickness of 10–15 μm were made by sandwiching a drop of dispersion between a larger and a smaller microscope cover slide (Chance, No. 1 thickness 170 μm). The samples were sealed with candle wax. Thin samples were clamped on all sides to prevent them from bending when the objectives were moved. Thicker samples were made in $0.1\times2\times50$ mm^3 capillaries (VitroCom, wall thickness 100 μm) that were closed by melting. The optical quality of the microscope cover slides is better than of the capillaries.
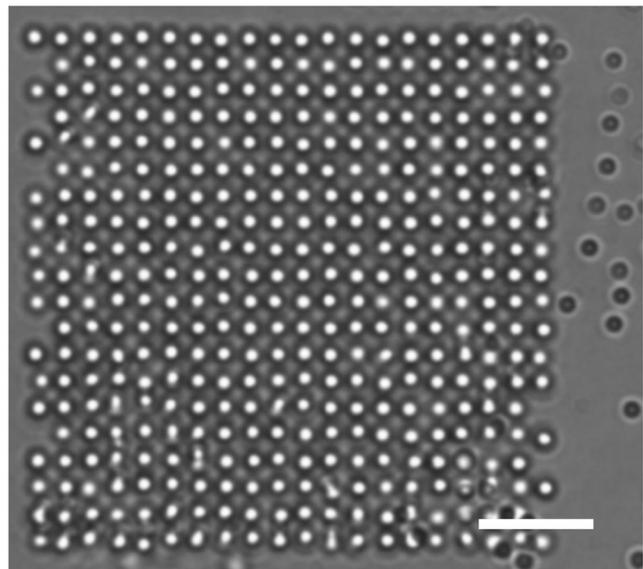

FIG. 3. Transmission microscopy image of 1.4 μm diam FITC–SiO_2 particles trapped in a time-shared array of 400 optical tweezers. The inverted objective was used for trapping as well as for imaging. Using the AODs the array was scanned at 96 Hz, well above the rolloff frequency of the particles in the traps. The particles on the right of the image were not trapped and were below the imaging plane. The scale bar is 10 μm.

III. DYNAMIC ARRAYS OF OPTICAL TWEEZERS

Figure 3 shows an array of 20×20 time-shared optical traps holding 1.4 μm FITC–SiO_2 particles. The inverted objective ($63\times$; 1.4 NA) was used for trapping as well as for imaging. The array was scanned at a frequency of 96 Hz using the AODs. The particles were dispersed in ethanol in a 100 μm thick capillary. The tweezers array was shifted up slightly with respect to the imaging plane. The (untrapped) particles next to the array were just below the imaging plane. Some traps held more than one particle while some traps on the edge of the pattern were not filled. The total laser power used to create the 400 traps was 1.0 W at the back focal plane of the trapping objective.

When time sharing a laser beam, the beam has to be scanned fast enough over the different positions in the sample for a particle to behave like it was trapped in a nontime-shared optical trap. In a single nontime-shared optical trap, a particle experiences a harmonic potential if its displacements from the center of the trap are not too large. The power spectrum of a particle's displacement in a harmonic potential is given by a Lorentzian[54]

$$S_x(f) = \frac{k_b T}{\gamma \pi^2 (f_c^2 + f^2)}, \qquad (1)$$

where k_b is Boltzmann's constant, T is temperature, and γ the viscous drag coefficient. For an isolated sphere of radius R in a solvent with dynamic viscosity η, the viscous drag coefficient is given by $\gamma=6\pi\eta R$. The rolloff frequency f_c is given by

$$f_c = \frac{\kappa}{2\pi\gamma}, \qquad (2)$$

where κ is the trap stiffness. For frequencies above f_c, the particle shows free diffusive behavior while for frequencies
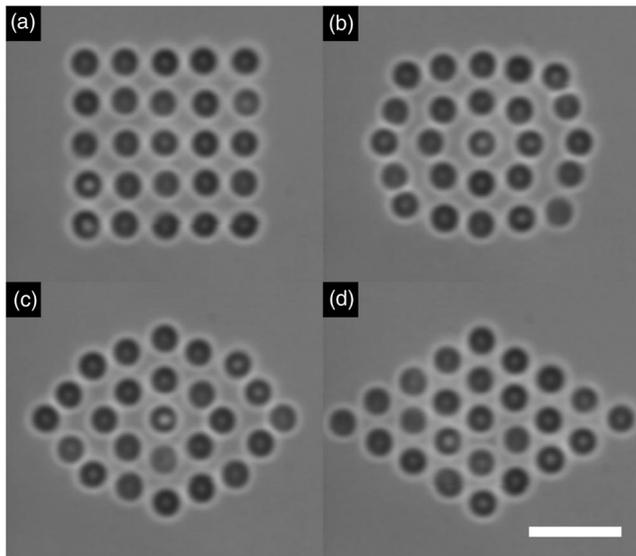
FIG. 4. (a) Transmission microscopy image of 1.4 μm diam FITC–SiO$_2$ particles in a time-shared array of 25 traps with square symmetry. The inverted objective was used for trapping as well as for imaging. Using the AODs, the pattern was dynamically changed in a few seconds without losing particles via intermediate patterns (b) and (c) to an array with triangular symmetry (d). The scale bar is 5 μm.

below f_c the optical trap confines the motion of the particle. Each trap in the array of tweezers in Fig. 3 was addressed 96 times/ps. The point-to-point scan frequency was 38.4 kHz. Using a quadrant photodiode on our setup as described elsewhere,[3] we measured the power spectrum of a 1.4 μm diam silica particle trapped in an optical trap created with a power of 2.5 mW at the back focal plane of the trapping objective. From this, the rolloff frequency was determined to be 10 Hz, which is well below the 96 Hz at which the array in Fig. 3 was scanned. Already hundreds of traps can be created by time sharing the AODs in a low viscosity solvent like ethanol for micron-size particles, and increasing the viscosity and thus lowering f_c, would allow even larger arrays to be made.

The maximum speed at which the position of an optical trap can be changed is determined by the width of the laser beam and the speed of the sound wave in the crystal. This is because the sound wave in the crystal has to be uniform in frequency over the laser beam to deflect the beam completely into a certain direction. In our setup it takes around 4.5 μs to change the direction in which the beam is diffracted, which sets the upper limit for point-to-point movement of the trap to 220 kHz. The maximum scanning speed can be increased by decreasing the width of the laser beam at the AODs and expanding the beam further after the AODs to keep the back focal plane of the objective overfilled.

Figure 4(a) shows 25 FITC–SiO$_2$ particles (1.4 μm diameter) trapped in a 5×5 square symmetric pattern using the inverted microscope objective (100×; 1.4 NA). The particles were dispersed in ethanol. The pattern was then changed in a few seconds, without losing particles from the trap, via intermediate stages [Figs. 4(b) and 4(c)] into the triangular pattern shown in Fig. 4(d). A *LabVIEW* program was used to switch between the different arrays of tweezers

in a few seconds. The maximum displacement of the trap in the sample is determined by the maximum deflection angle of the beam at the AODs, by the optics in the setup, and by the magnification of the microscope objective used. We used the (1,1) order of the diffracted beam after the AODs. For this order, a center frequency of 25 MHz on the AODs deflects the beam 45 mrad with respect to the zeroth order undiffracted beam. The position of the trap in the sample changes when the frequency on the AODs is changed around the center frequency. The accessible frequency interval ranges from 16 to 34 MHz corresponding to a deflection between −15 and +15 mrad of the beam at the AODs. The deflection angle at the back aperture of the objectives was reduced by a factor of 2.2 because of the telescope behind the AODs. The resulting maximum displacement of the optical traps in the sample was found to be 28, 45, and 71 μm in both the x and y direction for the 100×, 63×, and 40× objectives, respectively. For these objectives, the trapping force is comparable as they all have an NA of 1.4.

Compared to other techniques to time share optical tweezers, for example scanning mirrors,[16] AODs are fast and flexible. Even mirrors mounted on piezo scanners[17] have a scan rate of a few kHz, while the AODs can be used at hundreds of kHz. Other techniques that intensity share the beam, like diffractive optical elements[18,19] in combination with computer addressed spatial light modulators,[20,21] are very flexible although their computational process is complex and time consuming. Multiple tweezers generated with the generalized phase contrast method[55] are much faster than holographic optical tweezers but they only trap in two dimensions.

The AODs can also be used to create multiple tweezers without time sharing the laser beam. We used digital synthesizers to generate two frequency signals, which were combined as input for one of the AODs, while the other AOD had a single frequency as input. The laser beam was diffracted at different angles, and this was used to create multiple tweezers in the sample. Arrays of tweezers are possible using this approach although the intensities of the beams are interrelated, and higher order frequencies might appear. All arrays of tweezers in the remainder of the paper are created by time sharing the laser beam.

IV. OPTICAL TRAPPING AND DECOUPLED CONFOCAL IMAGING

The two microscope objectives on each side of the sample allow optical trapping and simultaneous three-dimensional imaging in the sample. To demonstrate this independent trapping and imaging, we created a three-dimensional structure of colloidal particles. The upright objective (100×; 1.4 NA) was used to create an array of eight optical traps. Each trap was filled with two 1.4 μm diam FITC–SiO$_2$ particles. The pair of particles in each trap was distributed along the propagation direction of the beam and formed a three-dimensional structure. This method was recently demonstrated, although not by imaging in three dimensions, by MacDonald and co-workers.[23] Using the inverted objective (63×; 1.4 NA) we imaged the
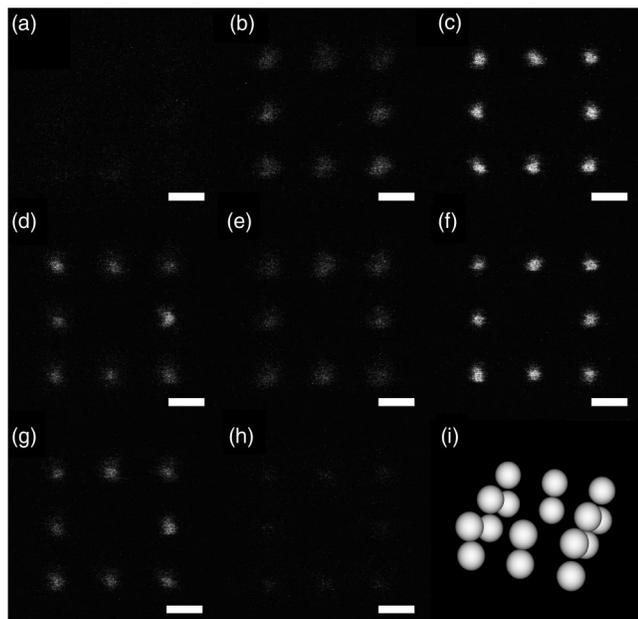
FIG. 5. (a)–(h) Fluorescence confocal images of a three-dimensional structure of colloidal particles created with a two-dimensional time-shared array of optical tweezers. Eight time-shared optical traps held two 1.4 μm diam FITC–SiO$_2$ particles each. The particles aligned on top of each other in the propagation direction of the laser beam. The height difference between each subsequent image was 546 nm with (a) below and (h) above the structure. The upright objective was used for trapping while the inverted objective was used for imaging. Only the fluorescent cores of the particles were imaged and image (i) was computer generated after determination of the particle coordinates from the confocal images. The scale bars are 2 μm.
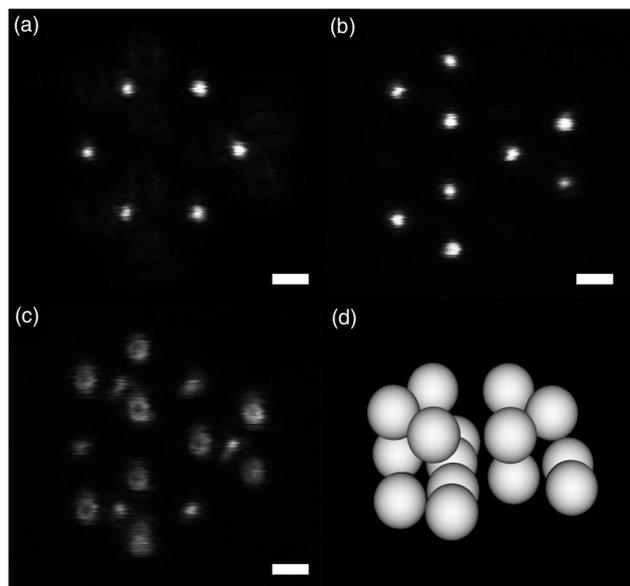

FIG. 6. Fluorescence confocal images of particles trapped in a three-dimensional array of tweezers created by synchronizing the Pockels cell and the AODs. (a) Six particles were trapped in the upper plane and (b) nine in the lower plane. (c) Between the two trapping planes fluorescence from particles in both planes was detected. The height difference between the two trapping planes was 1.7 μm. The upright objective was used for trapping while the inverted objective was used for imaging. The 1.4 μm diam FITC–SiO$_2$ particles were dispersed in ethanol, and only their fluorescent cores were imaged. (d) An image was computer generated on the basis of the confocal data. The scale bars are 1 μm.

sample in confocal mode. Starting below the structure and ending above it, we scanned through the two layers of particles.

Figure 5(a) shows a plane below the structure with almost no fluorescence signal detected. Moving upwards, the eight particles in the lower plane were imaged [Figs. 5(b) and 5(c)]. Between the two trapping planes [Figs. 5(d) and 5(e)] some fluorescence from the particles was detected. Moving further upwards, the particles in the second layer were imaged [Fig. 5(f)]. Finally, Fig. 5(h) shows a plane just above the structure [Fig. 5(h)]. Because the particles have a fluorescent core and non-fluorescent shell only the cores were imaged. The separation between the imaging planes in Fig. 5 was determined to be 546 nm.[56] From the confocal images we determined the three-dimensional coordinates of the particles, which we used to computer generate an image of the structure created by the optical traps [Fig. 5(i)].

V. ARRAYS OF TWEEZERS IN MORE THAN ONE PLANE USING ONE OBJECTIVE

We created two trapping planes, each with a different configuration of traps, using an (100×; 1.4 NA) upright objective. The three-dimensional array was then filled with 1.4 μm diam FITC–SiO$_2$ particles. The particles were dispersed in ethanol in a 10 μm thick sample. The lower objective (100×; 1.4 NA) was used for imaging. Figure 6(a) shows a confocal image of the upper plane in which six particles were trapped. The nine particles in the lower plane were imaged in Fig. 6(b). The distance between the trapping

planes was determined to be 1.7 μm.[56] When the confocal microscope was focused between the two trapping planes, both the upper and the lower plane were vaguely imaged [Fig. 6(c)]. From the confocal images we determined the position coordinates of the particles in the trapping array and generated an artificial image of the three-dimensional structure created [Fig. 6(d)].

VI. OPTICAL TWEEZERS IN CONCENTRATED DISPERSIONS

A. Tweezers-induced crystallization in concentrated colloidal dispersions

A 100 μm thick capillary was filled with 1.4 μm diam FITC–SiO$_2$ particles dispersed in DMF. The particles have a higher density than DMF ($\Delta\rho=1.05$ g/cm^3) and after sedimentation a height-dependent concentration profile formed at the bottom of the capillary. The number of particles in the sample was chosen such that the bottom layer of the sediment was still fluid-like. The sample was imaged with the confocal microscope using the inverted objective (100×; 1.4 NA). Figure 7(a) shows an image of the bottom layer. Only the fluorescent cores of the particles were visible, and, as can be seen, the particles were in the liquid state just below the freezing transition. The interparticle distance was 1.9 μm, due to a small charge on the particles. Figure 7(c) shows a scan through the sample orthogonal to the bottom layer and parallel to gravity. The sediment was only a few micrometers thick.

The beam was then focused into the sample from above (upright mode) using a low numerical aperture objective
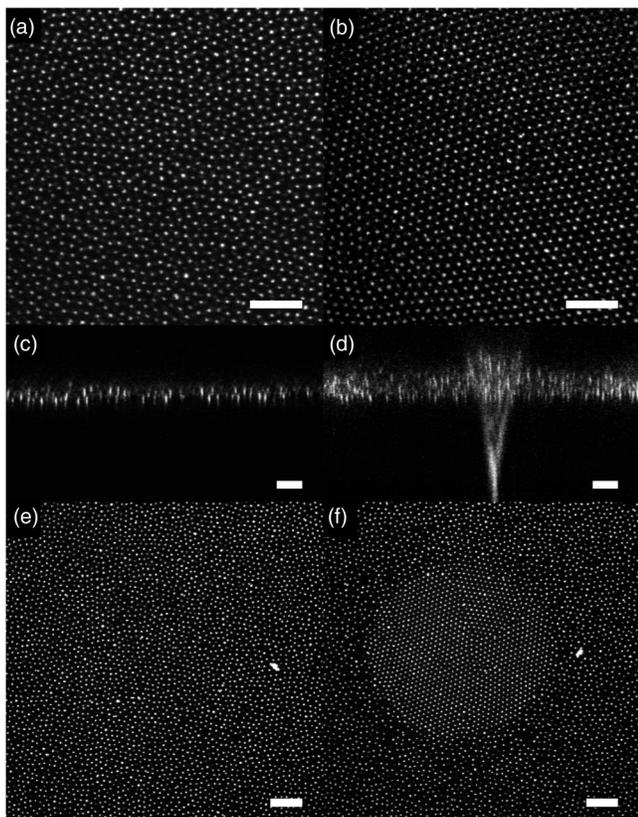
FIG. 7. Fluorescence confocal images of 1.4 μm diam FITC–SiO$_2$ particles dispersed in DMF. (a) In the absence of the optical tweezers the particles were in the bottom layer in a liquid state. (b) The bottom layer became crystalline when the trap was turned on, in the upright mode, using a low numerical aperture objective (20×; 0.7 NA). The crystal layer extended over hundreds of micrometers (c) A scan of the sample perpendicular to the bottom layer and in absence of the field. The sediment was a few particles thick (d) With the tweezers turned on the sediment became thicker. The trapping beam was imaged and the focus of the trap was 33 μm below the bottom plane of the sample. The size of the optical trap was diffraction limited and in the order a few particle diameters. (e) Bottom layer of a dispersion of 1.4 μm diam FITC–SiO$_2$ particles in ethanol. (f) A crystal formed when the laser was focused using a high numerical aperture objective (100×; 1.4 NA) in upright trapping mode. Scale bars are 10 μm.

(20×; 0.7 NA). With this low NA, three-dimensional trapping is not possible and the particles are pushed against the bottom of the sample cell. The focal plane of the upright objective was 33 μm below the bottom layer of the sediment. Figure 7(b) shows the bottom layer of the sample 15 min after the upright tweezers were turned on. The dispersion had crystallized due to the light field in the sample. The crystalline area extended over a few hundred micrometers. The defect lines in the crystal can be attributed to small aggregates in the dispersion from which they originate. Figure 7(d) shows an image scan parallel to gravity. The thickness of the sediment increased in comparison with the situation without tweezers [Fig. 7(c)]. The laser beam is visible in Fig. 7(d) as no infrared filter was used in front of the photomultiplier tubes. The laser power used was measured to be 0.58 W at the back focal plane of the objective. When the tweezers were turned off the crystal melted, and the sample returned to its original liquid state.

We also used a high numerical aperture objective (100×; 1.4 NA) to focus the laser in a dispersion of

1.4 μm diam FITC–SiO$_2$ particles dispersed in ethanol. Figure 7(e) shows a confocal image of particles in the fluid phase in the bottom layer of the sample before the laser was turned on. When the upright tweezers were turned on, a crystallite formed in the colloidal fluid [Fig. 7(f)]. The interparticle distance in the crystal was 1.6 μm. The diameter of the crystallite increased with the laser power used. For this experiment, the power at the back focal plane was measured to be 0.5 W. When the tweezers were turned off the crystallite melted within a few seconds and the sample returned to its original state.

The optical force on the particles in the bottom plane is proportional to the gradient of the intensity of the light field. The focused laser light applies an optical pressure towards the focal point. As particles were pushed towards the focal point, the concentration increased locally, and the thickness of the sediment increased. A steady state was achieved when the optical, the osmotic, and the gravitational pressure balanced. When the local pressure in the sample exceeded the pressure at the freezing transition, the colloidal fluid crystallized. Although the size of the focal spot was diffraction limited and in size only a few particle diameters, the gradient force far away from the focus was still large enough to crystallize the sample. Recently, Sullivan and co-workers reported crystallization of concentrated dispersions induced by increasing the volume fraction locally with gradients in electric fields.[57] Optical tweezers-induced crystallization can be viewed as a high-frequency analog of their technique. Crystallization of the layer of colloidal particles was not observed when the tweezers were operated in the inverted mode as no equilibrium situation was achieved and particles were pushed around through the sample. We are currently investigating the processes in more detail.

B. Manipulation of (core–shell) tracer particles in a concentrated dispersion

To demonstrate selective optical trapping in a concentrated dispersion, we dispersed a mixture of PS–SiO$_2$ tracer and FITC–SiO$_2$ host particles in a solvent mixture of DMF and DMSO with the same refractive index as SiO$_2$ at 1064 nm. The diameters of the particles were 975 and 1050 nm, respectively. The concentration of the samples was chosen such that, after the dispersion had sedimented in the 100 μm thick capillary, a thin sediment formed which was either liquid-like or crystalline in the bottom layer. We created a 3×3 square array of optical tweezers with different spacings between the traps in the bottom layer in the dispersion. Eight traps were filled with tracer particles, and one trap was left empty. The upright objective (63×; 1.4 NA) was used for trapping, while the inverted objective (100×; 1.4 NA) was used for imaging.

Figure 8 shows combined fluorescence and reflection confocal images of the trapped tracer particles surrounded by host particles. The tracer particles are displayed in black while the hosts are displayed in light gray. The images were averaged over multiple frames with a time step of 1.7 s between the frames. Because of the averaging, mobile particles were blurred in the images, while particles that were not moving were imaged sharply. Figure 8(a) was averaged over
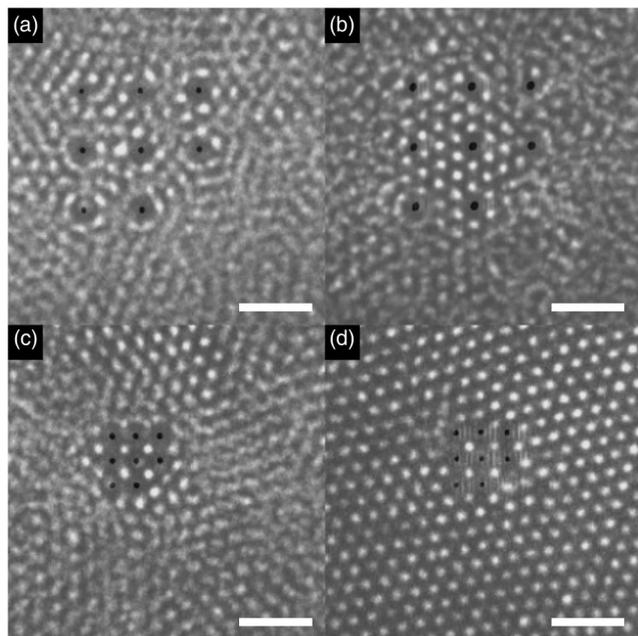
FIG. 8. Combined confocal reflection and fluorescence images of a mixture of PS–SiO$_2$ tracer particles (black) and FITC–SiO$_2$ host particles (light gray). The mixture was dispersed in a fluid matching the refractive index of the host particles. The tracer particles were trapped in a 3×3 array of optical tweezers. The upright objective was used for trapping while the inverted objective was used for imaging. The lattice spacing of the templates was (a) 4.1 μm, (b) 4.1 μm, (c) 1.6 μm, and (d) 1.8 μm. The template of tracer particles induced structure in the host dispersion. Images were averaged over (a) 20, (b) and (c) 10, and (d) four images with 1.7 s between the frames. Immobile particles were imaged sharply while moving particles became blurred. Only the cores of both tracer and host particles were imaged. Note that only eight of the nine traps were occupied and that no host particles are drawn towards nor expelled from the empty trap, demonstrating that optical forces on the host particles are negligible. Scale bars are 5 μm.

20 images and shows an open structure with a separation between the traps of 4.1 μm. The concentration of the surrounding host particles was below the freezing point, and they were in the liquid state. In the array with trapped tracer particles the host particles showed some ordering but did not crystallize. Figure 8(b) (averaged over ten frames) shows an array with the same trap separation as in Fig. 8(a), but here the host spheres crystallized with a hexagonal symmetry in the array with tracer particles. The host particles surrounding the array were still clearly liquid-like. Figures 8(c) and 8(d) (averaged over ten and four frames, respectively) show arrays with smaller trap separations of 1.6 and 1.8 μm. In Fig. 8(c) host spheres penetrate the array of tracer particles, resulting in an ordered structure with square symmetry while the surrounding host spheres were still liquid-like. Figure 8(d) shows that also in a crystalline layer the tracer particles can be trapped in an array that is incommensurate with the crystal lattice. The hexagonal layer incorporated the different symmetry of the trapped structure although some defect lines originate from the trapped structure. At the position of the empty trap in the 3×3 array can be seen that the force on the host particles was negligible compared to their thermal energy. If the host particles were either under or over matched by the solvent mixture, the optical forces on the host par-

ticles would either pull them towards or expel them from the trap.

The high index core of the tracer particles allowed them to be manipulated in a concentrated dispersion of refractive index matched host particles. The core-shell morphology of the tracer particles has several other advantages. Because the shell of the core-shell particles is of the same material as the host particles, all particles in the mixture have the same surface properties and thus the same interparticle interaction. Furthermore, the optically induced forces between trapped particles are decreased, as only the cores are trapped, and the forces decay strongly with interparticle distance.[22,58] Finally, the core–shell geometry is advantageous for trapping in three-dimensional arrays of optical traps (as in Secs. IV and V) as the scattering unit of a particle is smaller, thus giving less distortion of the laser field behind the particle.

VII. COUNTER-PROPAGATING TWEEZERS

Counterpropagating optical tweezers[1,47] have the advantage over single beam traps that they can trap strongly scattering particles. The scattering force on a particle is cancelled due to symmetry of the two beams along the optical axis. At the same time, the gradient force is added resulting therefore in stronger confinement of the particle in all directions compared to a single-beam trap.

To demonstrate such a counterpropagating trap, we trapped a 0.5 μm ZnS particle dispersed in ethanol. The high refractive index ($n_D^{20} = 2.0$) meant that the particle could not be trapped in a conventional single-beam gradient trap. Figure 9(a) shows on the left the ZnS particle in a counterpropagating trap. The trap was created using both the inverted and upright objective (both $100\times$; 1.4 NA). The laser power was divided equally between the lower and the upper beam path. The particle on the right in Fig. 9(a) is a 1.4 μm FITC–SiO$_2$ particle stuck to the lower sample wall. To demonstrate that the ZnS particle was indeed trapped in three dimensions in the counterpropagating trap, we moved the stage down in Figs. 9(b) and 9(c). As can be seen, the ZnS particle stayed in focus while the FITC–SiO$_2$ particle moved out of focus. We could shift the position of the ZnS particle with respect to the imaging plane by changing the relative power in the upper and lower beam paths. It should be noted that earlier counterpropagating traps used low NA lenses (and therefore radiation pressure) for trapping. As we use high NA objectives, particles are trapped by the gradient force.

VIII. DISCUSSION AND OUTLOOK

The setup described in this article was developed to both manipulate and image individual colloidal particles in three dimensions in concentrated colloidal dispersions. We have shown that the combination of confocal microscopy and time-shared optical tweezers allows independent three-dimensional imaging and manipulation of the dispersion. At present we are exploring, with the setup, the stability of three-dimensional arrangements of particles[23] and optically induced forces between noncore-shell particles[59] on a quantitative level.
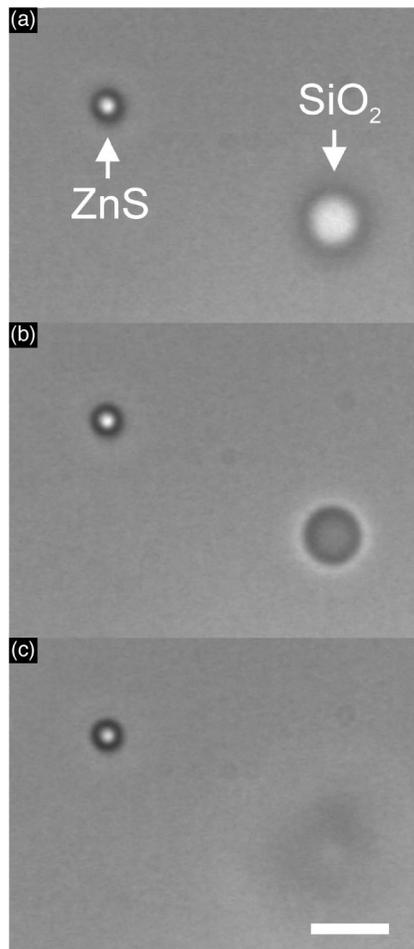
FIG. 9. (a) A 0.5 μm diam ZnS particle (left) trapped in counterpropagating optical tweezers next to a 1.4 μm diam FITC–SiO$_2$ particle (right) that was stuck to the surface of the sample cell. The ZnS particle was trapped in three dimensions as can be seen in (b) and (c) where the sample was moved down with respect to the trapping plane. The ZnS particle was trapped and therefore stayed in focus, while the FITC–SiO$_2$ particle moved out of the focal plane. It was not possible to trap the ZnS particle using single-beam optical tweezers. The scale bar is 2 μm.

By choosing AODs to timeshare the laser beam we have shown that it is possible to create large arrays of hundreds of optical traps and change them dynamically, because AODs can be scanned at hundreds of kHz. These arrays of tweezers were used to create two- and three-dimensional structures of particles. Arrays of tweezers in two planes were created using a Pockels cell and polarizing beam splitters. Such an approach does not make it possible to move particles in three dimensions, but is one of the fastest methods to create and dynamically change the symmetry of two independent two-dimensional arrays of optical tweezers.

In addition, we have shown that selective trapping and manipulation of individual tracer particles is possible if a concentrated system of host and tracer particles is used and the tracer particles have a core–shell geometry with a high refractive index material core and a lower index material shell. We have shown that when the host particles consist of the same material as the lower index shells, the tracer particles can be manipulated without exerting forces on the host particles. By fluorescently labeling the (cores of the) host

particles it is possible to follow the effects of the trapped spheres on the bulk dispersion on a single particle level in three dimensions. The optically trapped particles experience a local potential by which they can be brought out of equilibrium.

In combination with the use of the earlier mentioned arrays of tweezers we plan to study crystal nucleation. With our setup the umbrella-sampling scheme that uses a local potential to allow the possibility to probe unlikely events such as crystal nucleation in computer simulations,[60] can now be implemented experimentally.

Also without the use of a tracer–host system we have shown that it is possible to crystallize and melt colloidal dispersions using optical forces. In this case forces are exerted on collections of particles. By changing the numerical aperture of the lens the geometry of the volume on which forces are exerted can be changed. This technique bears strong resemblances with the use of gradients of low-frequency electric fields to manipulate the density of the colloidal dispersion.[57] In combination with a tracer–host system, this technique to manipulate the concentration can be used to study the critical nucleus size in a colloidal fluid close to crystallization as well.

Finally, by using counterpropagating traps high refractive index particles could be manipulated that could not be trapped in three dimensions with conventional single-beam optical tweezers. Recently, we have developed a method to create structures of colloidal particles on surfaces using single-beam optical tweezers.[37,38] Using the setup in counterpropagating mode allows particles with a high refractive index to be incorporated in such two- and three-dimensional structures giving the possibility to create or dope photonic materials with high index particles.

ACKNOWLEDGMENTS

[1] A. Ashkin, Phys. Rev. Lett. **24**, 156 (1970).
[2] A. Ashkin, J. M. Dziedzic, J. E. Bjorkholm, and S. Chu, Opt. Lett. **11**, 288 (1986).
[3] K. Visscher, S. P. Gross, and S. M. Block, J. Sel. Topics Quantum Electron **2**, 1066 (1996).
[4] D. G. Grier, Curr. Opin. Colloid Interface Sci. **2**, 264 (1997).
[5] K. Dholakia, G. Spalding, and M. MacDonald, Phys. World **15**, 31

(2002).

[6] D. G. Grier, Nature (London) **424**, 810 (2003).

[7] P. A. M. Neto and H. M. Nussenzveig, Europhys. Lett. **50**, 702 (2000).

[8] Y. Harada and T. Asakura, Opt. Commun. **124**, 529 (1996).

[9] A. Ashkin, in *Methods in Cell Biology*, edited by M. P. Sheetz (Academic, San Diego, 1998), Vol. 55, p. 1.

[10] K. Sasaki, M. Koshioka, H. Misawa, N. Kitamura, and H. Masuhara, Appl. Phys. Lett. **60**, 807 (1992).

[11] H. He, M. E. J. Friese, N. R. Heckenberg, and H. Rubinsztein-Dunlop, Phys. Rev. Lett. **75**, 826 (1995).

[12] K. Visscher, G. J. Brakenhoff, and J. J. Krol, Cytometry **14**, 105 (1993).

[13] M. E. J. Friese, T. A. Nieminen, N. R. Heckenberg, and H. Rubinsztein-Dunlop, Nature (London) **394**, 348 (1998).

[14] L. Paterson, M. P. MacDonald, J. Arlt, W. Sibbett, P. E. Bryant, and K. Dholakia, Science **292**, 912 (2001).

[15] J. Guck, R. Ananthakrishnan, T. J. Moon, C. C. Cunningham, and J. Kas, Phys. Rev. Lett. **84**, 5451 (2000).

[16] K. Sasaki, M. Koshioka, H. Misawa, N. Kitamura, and H. Masuhara, Opt. Lett. **16**, 1463 (1991).

[17] C. Mio, T. Gong, A. Terray, and D. W. M. Marr, Rev. Sci. Instrum. **71**, 2196 (2000).

[18] J.-M. Fournier, M. M. Burns, and J. A. Golovchenko, Proc. SPIE **2406**, 101 (1995).

[19] E. R. Dufresne and D. G. Grier, Rev. Sci. Instrum. **69**, 1974 (1998).

[20] Y. Hayasaki, M. Itoh, T. Yatagai, and N. Nishida, Opt. Rev. **6**, 24 (1999).

[21] J. Liesener, M. Reicherter, T. Haist, and H. J. Tiziani, Opt. Commun. **185**, 77 (2000).

[22] M. M. Burns, J.-M. Fournier, and J. A. Golovchenko, Science **249**, 749 (1990).

[23] M. P. MacDonald, L. Paterson, K. Volke-Sepulveda, J. Arlt, W. Sibbett, and K. Dholakia, Science **296**, 1101 (2002).

[24] M. Minsky, U. S. Patent No. 301467 (1961).

[25] J. K. Stevens, L. R. Mills, and J. E. Trogadis, *Three-dimensional Confocal Microscopy: Volume Investigation of Biological Systems* (Academic, San Diego, CA, 1994).

[26] M. H. Chestnut, Curr. Opin. Colloid Interface Sci. **2**, 158 (1997).

[27] A. van Blaaderen, Prog. Colloid Polym. Sci. **104**, 59 (1997).

[28] A. D. Dinsmore, E. R. Weeks, V. Prasad, A. C. Levitt, and D. A. Weitz, Appl. Opt. **40**, 4152 (2001).

[29] J. B. Pawley, *Handbook of Biological Confocal Microscopy* (Plenum, New York, 1995).

[30] A. van Blaaderen, K. P. Velikov, J. P. Hoogenboom, D. L. J. Vossen, A. Yethiraj, R. P. A. Dullens, T. van Dillen, and A. Polman, in *Photonic Crystals and Light Localization in the 21st Century*, edited by C. M. Soukoulis (Kluwer, Dordrecht, 2001), p. 239.

[31] M. Brunner, C. Bechinger, W. Strepp, V. Lobaskin, and H. H. von Grunberg, Europhys. Lett. **58**, 926 (2002).

[32] A. van Blaaderen, J. P. Hoogenboom, D. L. J. Vossen, A. Yethiraj, A. van der Horst, K. Visscher, and M. Dogterom, Faraday Discuss. **123**, 107 (2003).

[33] A. Yethiraj and A. van Blaaderen, Nature (London) **421**, 513 (2003).

[34] A. van Blaaderen and P. Wiltzius, Science **270**, 1177 (1995).

[35] W. K. Kegel and A. van Blaaderen, Science **287**, 290 (2000).

[36] U. Gasser, E. R. Weeks, A. Schofield, P. N. Pusey, and D. A. Weitz, Science **292**, 258 (2001).

[37] J. P. Hoogenboom, D. L. J. Vossen, C. Faivre-Moskalenko, M. Dogterom, and A. van Blaaderen, Appl. Phys. Lett. **80**, 4828 (2002).

[38] D. L. J. Vossen, J. P. Hoogenboom, K. Overgaag, and A. van Blaaderen, Mater. Res. Soc. Symp. Proc. **705**, y6.8.1 (2002).

[39] J. C. Crocker and D. G. Grier, Phys. Rev. Lett. **73**, 352 (1994).

[40] J. C. Crocker, J. A. Matteo, A. D. Dinsmore, and A. G. Yodh, Phys. Rev. Lett. **82**, 4352 (1999).

[41] S. Henderson, S. Mitchell, and P. Bartlett, Colloids Surf., A **190**, 81 (2001).

[42] P. T. Korda and D. G. Grier, J. Chem. Phys. **114**, 7570 (2001).

[43] J. Leach, G. Sinclair, P. Jordan, J. Courtial, M. J. Padgett, J. Cooper, and Z. J. Laczik, Opt. Express **12**, 220 (2004).

[44] A. Resnick, Rev. Sci. Instrum. **72**, 4059 (2001).

[45] A. Hoffmann, G. M. Z. Horste, G. Pilarczyk, S. Monajembashi, V. Uhl, and K. O. Greulich, Appl. Phys. B: Lasers Opt. **71**, 747 (2000).

[46] K. Visscher and G. J. Brakenhoff, Cytometry **12**, 486 (1991).

[47] S. B. Smith, Y. J. Cui, and C. Bustamante, Science **271**, 795 (1996).

[48] J. C. Crocker and D. G. Grier, J. Colloid Interface Sci. **179**, 298 (1996).

[49] A. van Blaaderen and A. Vrij, Langmuir **8**, 2921 (1992).

[50] N. A. M. Verhaegh and A. van Blaaderen, Langmuir **10**, 1427 (1994).

[51] H. Giesche, J. Eur. Ceram. Soc. **14**, 205 (1994).

[52] K. P. Velikov and A. van Blaaderen, Langmuir **17**, 4779 (2001).

[53] C. Graf, D. L. J. Vossen, A. Imhof, and A. van Blaaderen, Langmuir **19**, 6693 (2003).

[54] F. Gittes and C. F. Schmidt, in *Methods in Cell Biology*, edited by M. P. Sheetz (Academic, San Diego, 1998), Vol. 55, p. 129.

[55] R. L. Eriksen, V. R. Daria, and J. Gluckstad, Opt. Express **10**, 597 (2002).

[56] S. W. Hell and E. H. K. Stelzer, in *Handbook of Biological Confocal Microscopy*, edited by J. B. Pawley (Plenum, New York, 1995).

[57] M. Sullivan, K. Zhao, C. Harrison, R. H. Austin, M. Megens, A. Hollingsworth, W. B. Russel, Z. D. Cheng, T. Mason, and P. M. Chaikin, J. Phys.: Condens. Matter **15**, S11 (2003).

[58] M. I. Antonoyiannakis and J. B. Pendry, Europhys. Lett. **40**, 613 (1997).

[59] R. C. Gauthier and M. Ashman, Appl. Opt. **37**, 6421 (1998).

[60] S. Auer and D. Frenkel, Nature (London) **409**, 1020 (2001).